*Inorg. Chem.* **2008**, *47*, 10419−10424

# On the Strongly Correlated Electron Hydride $Ce_2Ni_2MgH_{7.7}$

**Bernard Chevalier,*,† Aleksandra A. Krolak,† Jean-Louis Bobet,† Etienne Gaudin,† François Weill,† Wilfried Hermes,‡ and Rainer Pöttgen‡**

*CNRS, Université de Bordeaux, ICMCB, 87 avenue du Docteur Albert Schweitzer, 33608 Pessac Cedex, France, and Institut für Anorganische and Analytische Chemie, Westfälische Wilhelms-Universität Münster, Corrensstrasse 30, 48149 Münster, Germany*

Received June 11, 2008

The intermediate valence compound $Ce_2Ni_2Mg$ absorbs irreversibly hydrogen when exposed under 1 MPa of $H_2$ pressure at room temperature. The resulting hydride $Ce_2Ni_2MgH_{7.7}$ is stable in air and crystallizes as the deuteride $La_2Ni_2MgD_8$ in a monoclinic structure (space group $P2_1/c$) with the unit cell parameters $a = 11.7620(2)$, $b = 7.7687(2)$, and $c = 11.8969(2)$ Å and $\beta = 92.75°$. The H-insertion in $Ce_2Ni_2Mg$ induces a structural transition from a tetragonal to a monoclinic symmetry with an unit cell volume expansion $\Delta V_m/V_m \approx 24.9\%$. The investigation of the hydride by magnetization, electrical resistivity, and specific heat measurements indicates a change from an intermediate valence behavior to a non-magnetic strongly correlated electron system. This transition results from a change of the coupling constant $J_{cf}$ between 4f(Ce) and conduction electrons induced by the hydrogenation.

## Introduction

In recent years, several works were devoted to a change of the valence state of cerium caused by hydrogenation of the intermetallics CeMX (M = transition metal and X = p-element). In some cases, the hydrogen insertion into an intermediate valence compound preserves the crystal symmetry of the intermetallic but induces the appearance of a magnetically ordered state. For instance, the hydrogenation of the intermediate valence indide CeNiIn leads to a ferromagnet $CeNiInH_{1.8}$.[1−3] This behavior was explained using the Doniach phase diagram highlighting the competition between the Rudermann−Kittel−Kasuya−Yosida (RKKY) indirect magnetic interaction and the Kondo effect, governed by the strength of the constant coupling $J_{cf}$ between 4f(Ce) and conduction electrons.[4] Generally, the hydrogenation induces an increase of the unit cell volume $V_m$ leading to a decrease of $J_{cf}$ favoring a magnetic ordering. It was clearly demonstrated by electronic structure calculations that the 4f(Ce) states are more localized in the hydride $CeNiInH_{1.8}$ than those existing in the pristine compound CeNiIn.[3] But if the hydrogen insertion is smaller (weak increase of $V_m$), only a transition from intermediate valence to magnetic behavior without long-range order is evidenced as for the heavy-fermion system $CeNiInH_{0.6}$[2] and the nearly Ce-trivalent hydrides $CeRhSnH_{0.8}$ and $CeIrSnH_{0.7}$.[5]

On the contrary, if the pristine intermetallic is close to a pure trivalent state, a small hydrogen insertion can induce the occurrence of a magnetically ordered state. For instance, the hydrogenation of the ternary stannide CeNiSn, which is considered as an anisotropic dense Kondo compound,[6] leads to the antiferromagnetic hydride CeNiSnH.[7−12] In this case, a small increase of $V_m$ (around 3%) is sufficient to obtain a hydride having a Néel temperature of 4.5 K.

Two years ago, it was reported that the ternary compound $La_2Ni_2Mg$, which crystallizes in the tetragonal $Mo_2FeB_2$ structure type, rapidly absorbs hydrogen at 373 K.[13] The resulting hydride $La_2Ni_2MgH_8$ presents a new monoclinic structure which results from a distortion of the tetragonal $Mo_2FeB_2$ type. Considering these results, it is interesting to perform hydrogenation of $Ce_2Ni_2Mg$ which is isotypic to

* To whom correspondence should be addressed. E-mail: chevalier@icmcb-bordeaux.cnrs.fr. Fax: +33 5 4000 2761. Phone: +33 4000 6336.
† ICMCB, CNRS, Université de Bordeaux.
‡ Institut für Anorganische and Analytische Chemie, Westfälische Wilhelms-Universität Münster.

(1) Chevalier, B.; Kahn, M. L.; Bobet, J.-L.; Pasturel, M.; Etourneau, J. *J. Phys.: Condens. Matter* **2002**, *14*, L365–368.
(2) Shashikala, K.; Sathyamoorthy, A.; Raj, P.; Dhar, S. K.; Malik, S. K. *J. Alloys Compd.* **2007**, *437*, 7–11.
(3) Matar, S. F.; Chevalier, B.; Eyert, V.; Etourneau, J. *Solid State Sci.* **2003**, *5*, 1385–1393.
(4) Chevalier, B.; Wattiaux, A.; Bobet, J.-L. *J. Phys.: Condens. Matter* **2006**, *18*, 1743–1755.
(5) Chevalier, B.; Sebastian, C. P.; Pöttgen, P. *Solid State Sci.* **2006**, *8*, 1000–1008.
(6) Takabatake, T.; Teshima, F.; Fujii, H.; Nishigori, S.; Suzuki, T.; Fujita, T.; Yamaguchi, Y.; Sakurai, J.; Jaccard, D. *Phys. Rev. B* **1990**, *41*, 9607–9610.

10.1021/ic801076b CCC: $40.75 
Published on Web 10/22/2008

$La_2Ni_2Mg$.[14] This compound based on cerium is considered as an intermediate valence system resulting from a strong $J_{cf}$ interaction between 4f(Ce) and conduction electrons.[15]

During our systematic studies devoted to the influence of hydrogenation on the cerium valence in intermetallics, we have succeeded to incorporate hydrogen into $Ce_2Ni_2Mg$. Herein we report on the structural, transport, thermal, and magnetic properties of the hydride $Ce_2Ni_2MgH_{7.7}$. Our investigation shows that this hydride presents an enhanced specific heat at low temperatures but no magnetic ordering is evident above 1.8 K.

## Experimental Section

**Synthesis of $Ce_2Ni_2Mg$ and its Hydride.** Starting materials for the synthesis of $Ce_2Ni_2Mg$ were a cerium ingot (>99.9%), nickel wire (>99.9%), and a magnesium rod (>99.95%). The elements (2:2:1 atomic ratio) were introduced in a small tantalum tube arc-welded under an argon pressure (600 mbar).[16] The argon was purified over molecular sieves, silica gel, and titanium sponge (900 K). The tantalum tube was placed in a water-cooled quartz sample chamber[17] of a high-frequency furnace, first heated for 2 min at 1300 K and subsequently annealed for 2 h at 920 K, followed by quenching. The temperature was controlled through a Sensor Therm Metis MS09 pyrometer with an accuracy of ±30 K. The reaction product was checked by X-ray powder diffraction (Guinier technique) using Cu $K\alpha_1$ radiation and α-quartz as an internal standard. The experimental pattern matched a calculated one[18] indicating pure $Ce_2Ni_2Mg$ on the level of X-ray powder diffraction.

Hydrogen sorption properties of $Ce_2Ni_2Mg$ were investigated with the use of an automatic Sievert-type volumetric apparatus (HERA, Hydrogen Storage System[19]) at room temperature. Before absorption, the sample (approximately 400 mg of powder) was heated at 473 K under dynamic vacuum for 2 h. Then, the sample was cooled down to room temperature and the hydrogen was introduced up to 1 MPa. The amount of hydrogen absorbed is deduced from the variation of the pressure in a calibrated volume (according to the Sievert method).

Figure 1 presents the first hydrogen absorption kinetic of $Ce_2Ni_2Mg$ performed at room temperature under a constant pressure of $P(H_2) = 1$ MPa. The amount of hydrogen absorbed increases very slowly during the first 50 ks (≈ 14 h) of hydrogenation (i.e., corresponding to the activation step), then more rapidly (absorption and diffusion step), and finally shows saturation after 110 ks (≈ 30−35 h). The composition $Ce_2Ni_2MgH_{7.7(2)}$ is attained; the corresponding weight capacity is around 1.84 wt %. This hydrogen content agrees well with the one determined by hydrogenation for the isotypic ternary compound $La_2Ni_2Mg$.[13] The resulting hydride is stable in ambient conditions since no hydrogen desorption is observed at room temperature after its treatment under a low hydrogen pressure ($P(H_2) = 1$ kPa) or dynamic vacuum.

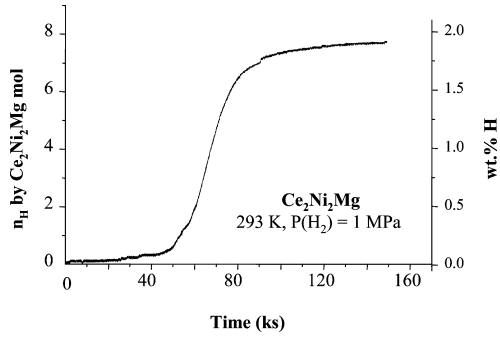


**Figure 1.** First hydrogen absorption at room temperature (293 K) and a hydrogen pressure of $P(H_2) = 1$ MPa for $Ce_2Ni_2Mg$. The number of hydrogen atoms inserted is expressed by $Ce_2Ni_2Mg$ mol or weight percentage.

**Powder Diffraction Measurements of the Hydride.** Electron diffraction experiment was performed on a JEOL 2000FX microscope equipped with a double tilt specimen holder. Prior to the observation, the powder was crushed in ethanol and a drop of the suspension was deposited on a copper grid with a carbon film. The crystal structure of the hydride $Ce_2Ni_2MgH_{7.7}$ was determined using X-ray powder diffraction. The data were collected with a Philips X-Pert diffractometer operating at room temperature and using Cu Kα radiation. The powder diffraction pattern was scanned over the angular range 12−130° with a step size of $\Delta(2\theta) = 0.008°$. Rietveld refinement was performed using the Jana2000 program package[20] in the 12−130° range. The initial atomic coordinates were taken from the previous study of the isotypic hydride $La_2Ni_2MgH_8$.[13] The background was estimated by a Legendre polynomial and the peak shape was described by a Lorentz function varying two profile coefficients. The refinement of peak asymmetry was performed using the Simpson parameter in Jana2000.[20] A single sharp peak was observed at 92.5°. Since no other peaks with the same shape were observed in the powder pattern (see for instance the zoom in figure 2) it was not possible to explain its presence. Thus, the zone around 92.5° peak, considered as an artifact, was excluded from the refinement. The isotropic Atomic Displacement Parameters (ADPs) of the magnesium positions (lightest element) were constrained to be equal. The reliability factors determined at the end of the refinement were $R_p/R_{wp} = 3.07/4.24\%$, $R_F = 2.24\%$, and $R_B = 4.53\%$. The simulated and experimental patterns are displayed in Figure 2 and the atomic positions with the isotropic ADPs are gathered in Table 1.

**Electrical Resistivity, Magnetization, and Specific Heat Measurements.** For electrical resistivity measurements, the hydride was compacted manually at room temperature (compactness ≅ 80%) to form a polycrystalline pellet (diameter = 6 mm and thickness = 3 mm) and then a bar of 1.5 × 1.5 × 5 $mm^3$ was cut from the pellet. These measurements were carried out above 4.2 K

(7) Yartys, V. A.; Ouladdiaf, B.; Isnard, O.; Khyzhun, O. Yu.; Buschow, K. H. J. *J. Alloys Compd.* **2003**, *359*, 62–65.
(8) Stange, M.; Paul-Boncour, V.; Latroche, M.; Percheron-Guégan, A.; Isnard, O.; Yartys, V. A. *J. Alloys Compd.* **2005**, *404−406*, 144–149.
(9) Chevalier, B.; Wattiaux, A.; Fournès, L.; Pasturel, M. *Solid State Sci.* **2004**, *6*, 573–577.
(10) Chevalier, B.; Pasturel, M.; Bobet, J.-L.; Etourneau, J.; Isnard, O.; Sanchez Marcos, J.; Rodriguez Fernandez, J. *J. Magn. Magn. Mater.* **2004**, *272−276*, 576–578.
(11) Chevalier, B.; Pasturel, M.; Bobet, J.-L.; Decourt, R.; Etourneau, J.; Isnard, O.; Sanchez Marcos, J.; Rodriguez Fernandez, J. *J. Alloys Compd.* **2004**, *383*, 4–9.
(12) Sanchez Marcos, J.; Rodriguez Fernandez, J.; Chevalier, B. *J. Magn. Magn. Mater.* **2007**, *310*, 383–385.
(13) Chotard, J.-N.; Filinchuk, Y.; Revaz, B.; Yvon, K. *Angew. Chem.* **2006**, *118*, 7934–7937.
(14) Hoffmann, R.-D.; Fugmann, A.; Rodewald, U. Ch.; Pöttgen, R. *Z. Anorg. Allg. Chem.* **2000**, *626*, 1733–1738.
(15) Geibel, C.; Klinger, U.; Weiden, M.; Buschinger, B.; Steglich, F. *Physica B* **1997**, *237−238*, 202–204.
(16) Pöttgen, R.; Gulden, Th.; Simon, A. *GIT Labor-Fachzeitschrift* **1999**, *43*, 133–136.
(17) Kuβmann, D.; Hoffmann, R.-D.; Pöttgen, R. *Z. Anorg. Allg. Chem.* **1998**, *624*, 1727–1735.
(18) Yvon, K.; Jeitschko, W.; Parthé, E. *J. Appl. Crystallogr.* **1977**, *10*, 73–74.
(19) Schulz, R.; Boily, S.; Huot, J. *Hydro-Quebec Patent No. WO98/00505*, 1998.
(20) Petricek, V.; Dusek, M. *The crystallographic computing system Jana*; Institute of Physics: Praha, Czech Republic, 2000.

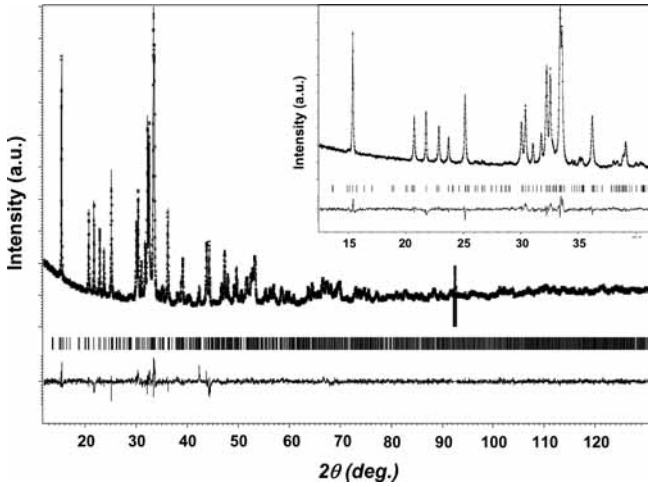


**Figure 2.** Observed (cross), calculated (solid line), and difference (bottom) X-ray powder diffraction patterns for $Ce_2Ni_2MgH_{7.7}$. The inset shows a zoom-in view of the low-angle region of the pattern.

**Table 1.** Atomic Coordinates and Isotropic Displacement Parameters for the Metal Sites of $Ce_2Ni_2MgH_{7.7}$, Space Group $P2_1/c$

| position | $x$ | $y$ | $z$ | $U_{iso}$ (Å$^2$) |
|---|---|---|---|---|
| Ce1 | 0.8361(4) | 0.6622(6) | 0.6807(3) | 0.0079(13) |
| Ce2 | 0.6032(4) | 0.6676(7) | 0.4151(3) | 0.024(2) |
| Ce3 | 0.8990(3) | 0.1576(6) | 0.6125(3) | 0.0095(15) |
| Ce4 | 0.6621(4) | 0.3232(6) | 0.8432(3) | 0.015(2) |
| Ni1 | 0.8473(6) | 0.8559(15) | 0.4616(6) | 0.002(3) |
| Ni2 | 0.3168(8) | 0.650(2) | 0.4164(7) | 0.004(3) |
| Ni3 | 0.0542(9) | 0.643(2) | 0.1532(7) | 0.023(4) |
| Ni4 | 0.5707(9) | 0.875(2) | 0.1793(7) | 0.036(5) |
| Mg1 | 0.895(2) | 0.506(3) | 0.4073(13) | 0.008(4)[a] |
| Mg2 | 0.624(2) | 0.537(3) | 0.123(2) | 0.008(4)[a] |

[a] Constrained to be equal.

using the standard dc four probes method with silver paint contacts and an intensity current of 10 mA. The magnetization measurements were performed on a part of the pellet using a superconducting quantum interference device magnetometer in the temperature range of 1.8−300 K and applied fields up to 4.6 T. For the matter of comparison, similar measurements were performed on a block of the initial ternary compound $Ce_2Ni_2Mg$.

Heat capacity measurements on the hydride were performed by a relaxation method with a Quantum Design PPMS system and using a two tau model analysis. Data were taken in the 1.8−50 K temperature range. For these latter measurements, the sample was a plate of 18.1 mg weight obtained from the same pellet used for the electrical resistivity and magnetization measurements.

## Results and Discussion

**Structural Properties.** The electron diffraction patterns obtained on the hydride $Ce_2Ni_2MgH_{7.7}$ (Figure 3) can be fully indexed using a monoclinic cell as the one used to describe the structure of the deuteride $La_2Ni_2MgD_8$.[13] Its examination by X-ray powder diffraction confirms the unit cell parameters $a = 11.7620(2)$, $b = 7.7687(2)$, and $c = 11.8969(2)$ Å and $\beta = 92.748(2)°$. The $a$, $b$, and $c$ parameters are smaller than those reported for $La_2Ni_2MgD_8$ in agreement with the lanthanoid contraction.

$Ce_2Ni_2Mg$ crystallizes with the $Mo_2FeB_2$ structure, an ordered variant of the tetragonal $U_3Si_2$ type structure. After insertion of hydrogen atoms, a monoclinic distortion of the unit-cell is observed for $Ce_2Ni_2MgH_{7.7}$. The cell vectors $\mathbf{a_t}$, $\mathbf{b_t}$, $\mathbf{c_t}$ of the tetragonal cell and $\mathbf{a_m}$, $\mathbf{b_m}$, $\mathbf{c_m}$ of the ideal monoclinic unit cell are related with the following relationship: $\mathbf{a_m} = \mathbf{a_t} + 2\mathbf{c_t}$, $\mathbf{b_m} = \mathbf{b_t}$ and $\mathbf{c_m} = -\mathbf{a_t} + 2\mathbf{c_t}$. The volume of the ideal monoclinic cell is four times greater than that of the tetragonal cell. In going from $Ce_2Ni_2Mg$ to $Ce_2Ni_2MgH_{7.7}$, an increase in the unit cell volume $V_m$ per formula unit (108.68 Å$^3$ taken from ref 21 → 135.73 Å$^3$) of

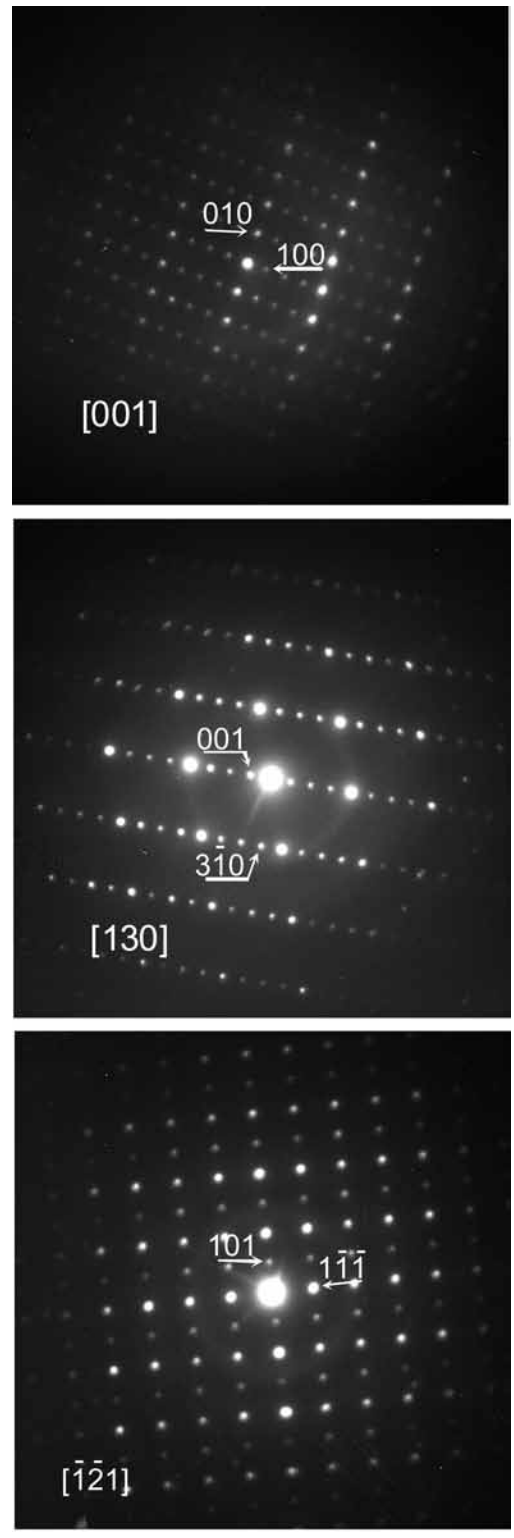


**Figure 3.** Electron diffraction patterns obtained on the hydride $Ce_2Ni_2MgH_{7.7}$ and the indexing with a monoclinic cell.

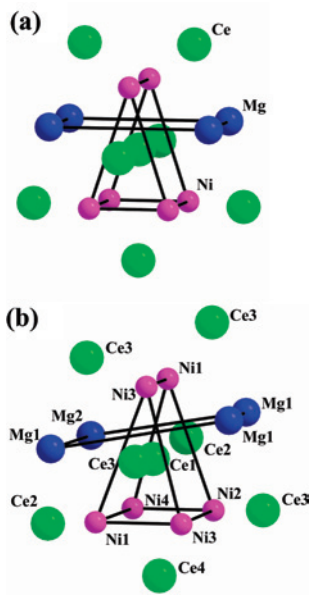


**Figure 4.** First coordination sphere of (a) Ce atoms in $Ce_2Ni_2Mg$ and (b) Ce1-position in $Ce_2Ni_2MgH_{7.7}$.

around 24.9% is observed. Similar increase is detected during the hydrogenation of $La_2Ni_2Mg$ but the reported value was smaller (20.3%).[13]

The structure of $Ce_2Ni_2MgH_{7.7}$ is formed along the [101] direction of infinite columns of tetragonal prisms of Ce atoms filled by Mg atoms (CsCl-type columns) and infinite columns of trigonal prisms of Ce atoms filled by Ni atoms ($AlB_2$-type columns). To better understand the change in physical properties induced by the cell expansion it is interesting to analyze the first coordination sphere of the Ce atoms. In $Ce_2Ni_2Mg$, the Ce atoms are located in a trigonal prism of Ni atoms (Figure 4a). They are also surrounded by a square of Mg atoms and by seven Ce atoms (Table 2). In this intermetallic, the distances Ce−Ni vary from 2.899 to 2.949 Å with an average value of 2.932 Å, and the distance Ce−Mg is equal to 3.387 Å.[21] On the contrary, in hydride $Ce_2Ni_2MgH_{7.7}$, the first coordination sphere of Ce is strongly expanded and distorted. The distortion of the near neighbor coordination of Ce1 is shown in Figure 4b and is similar to those of the other Ce positions. For this last compound, the Ce−Ni distances vary from 2.951 to 3.556 Å, and the average Ce−Ni distances for each cerium positions are $d_{Ce1-Ni}$ = 3.169, $d_{Ce2-Ni}$ = 3.262, $d_{Ce3-Ni}$ = 3.090, and $d_{Ce4-Ni}$ = 3.254 Å (Table 2). The same observation can be done for the Ce−Mg distances. In $Ce_2Ni_2Mg$, the Ce−Mg distance is always 3.387 Å whereas in its hydride, the average distance is 3.61, 3.65, 3.63, and 3.75 Å, respectively, for the Ce1, Ce2, Ce3, and Ce4 atoms. This comparison suggests a modification of the Ce-valence induced by the hydrogen insertion into $Ce_2Ni_2Mg$ through a significant increase of the interatomic distances $d_{Ce-Ni}$ and $d_{Ce-Mg}$ in the sequence $Ce_2Ni_2Mg \rightarrow Ce_2Ni_2MgH_{7.7}$. A relationship between the Ce valence and the distances $d_{Ce-Ni}$ for binary or ternary compounds in the Ce−Ni−Sn system was reported by

(21) Pöttgen, R.; Fugmann, A.; Hoffmann, R.-D.; Rodewald, Ute Ch.; Niepmann, D. *Z. Naturforsch.* **2000**, *55b*, 155–161.

**Table 2.** Selected Interatomic Distances (Å) in $Ce_2Ni_2MgH_{7.7}$ and $Ce_2Ni_2Mg$[21]

| $Ce_2Ni_2MgH_{7.7}$ | | | | | | $Ce_2Ni_2Mg$ | | |
|---|---|---|---|---|---|---|---|---|
| Ce1 | Ni3 | 3.010(13) | Ce3 | Ni2 | 2.951(12) | Ce | Ni | 2.899 |
| | Ni1 | 3.019(8) | | Ni3 | 2.989(14) | | Ni | 2.899 |
| | Ni4 | 3.134(12) | | Ni1 | 2.996(9) | | Ni | 2.949 |
| | Ni2 | 3.202(14) | | Ni1 | 3.154(8) | | Ni | 2.949 |
| | Ni3 | 3.309(13) | | Ni3 | 3.213(11) | | Ni | 2.949 |
| | Ni1 | 3.341(8) | | Ni3 | 3.236(9) | | Ni | 2.949 |
| | Mg2 | 3.46(2) | | Mg2 | 3.58(2) | | Mg | 3.387 |
| | Mg1 | 3.574(15) | | Mg1 | 3.58(2) | | Mg | 3.387 |
| | Mg1 | 3.62(2) | | Mg1 | 3.65(2) | | Mg | 3.387 |
| | Mg1 | 3.77(2) | | Mg1 | 3.729(14) | | Mg | 3.387 |
| | Ce3 | 3.876(6) | | Ce1 | 3.876(5) | | Ce | 3.685 |
| | Ce4 | 3.904(6) | | Ce1 | 4.009(7) | | Ce | 3.767 |
| | Ce3 | 4.009(7) | | Ce1 | 4.078(7) | | Ce | 3.767 |
| | Ce3 | 4.078(7) | | Ce4 | 4.147(5) | | Ce | 3.767 |
| | Ce2 | 4.082(6) | | Ce4 | 4.205(6) | | Ce | 3.767 |
| | Ce2 | 4.214(6) | | Ce3 | 4.406(6) | | Ce | 3.981 |
| | Ce3 | 4.988(6) | | Ce1 | 4.988(6) | | Ce | 3.981 |
| Ce2 | Ni4 | 3.202(9) | Ce4 | Ni2 | 3.117(9) | | | |
| | Ni4 | 3.224(14) | | Ni4 | 3.142(13) | | | |
| | Ni4 | 3.242(11) | | Ni2 | 3.160(11) | | | |
| | Ni1 | 3.246(9) | | Ni4 | 3.202(14) | | | |
| | Ni2 | 3.288(14) | | Ni3 | 3.345(12) | | | |
| | Ni2 | 3.372(11) | | Ni1 | 3.556(9) | | | |
| | Mg2 | 3.37(2) | | Mg2 | 3.58(2) | | | |
| | Mg2 | 3.64(2) | | Mg2 | 3.77(2) | | | |
| | Mg1 | 3.66(2) | | Mg1 | 3.80(2) | | | |
| | Mg2 | 3.93(2) | | Mg2 | 3.84(2) | | | |
| | Ce4 | 3.976(7) | | Ce1 | 3.904(6) | | | |
| | Ce1 | 4.082(6) | | Ce2 | 3.976(7) | | | |
| | Ce4 | 4.113(7) | | Ce2 | 4.113(7) | | | |
| | Ce2 | 4.150(7) | | Ce3 | 4.147(5) | | | |
| | Ce1 | 4.214(6) | | Ce3 | 4.205(6) | | | |
| | Ce4 | 4.274(6) | | Ce2 | 4.274(6) | | | |
| | Ce4 | 4.509(6) | | Ce2 | 4.509(6) | | | |

Chevalier et al.[22] They have shown that for Ce in the intermediate valence, the $d_{Ce-Ni}$ distances vary from 2.806 to 2.890 Å and for Ce in the trivalent state it varies from 3.027 to 3.522 Å. One can note that according to their analysis, the $d_{Ce-Ni}$ distances observed in $Ce_2Ni_2Mg$ and $Ce_2Ni_2MgH_{7.7}$ correspond to a Ce in an intermediate and a trivalent state, respectively. This is in complete agreement with the physical characterization of the hydride presented in the following.

**Physical Properties.** In Figure 5, the temperature dependences of the magnetic susceptibility $\chi_m$ of $Ce_2Ni_2Mg$ and its hydride are compared. The curve $\chi_m = f(T)$ relative to the initial intermetallic presents some features (inset of Figure 5): (i) there is no evidence for Curie−Weiss dependence; (ii) the presence of a broad maximum around 190−210 K is a characteristic of valence fluctuating systems,[23] and (iii) the increase of $\chi_m$ below 60−55 K appears to originate from a small amount of free $Ce^{3+}$ ions stabilized owing to lattice defects as is often observed in other valence fluctuating systems.[24] The curve $\chi_m = f(T)$ reported here for $Ce_2Ni_2Mg$ is in relatively good agreement with that determined by Geibel et al.[15] According to the model proposed by Lawrence et al.[23] for the intermediate valence compounds, $\chi_m$ of $Ce_2Ni_2Mg$ can be expressed at low temperatures (<55 K) by $\chi_m = \chi_m(0) + nC/T$ where $\chi_m(0)$ is the magnetic

(22) Chevalier, B.; Etourneau, J. *J. Mater. Chem.* **1999**, *9*, 1789–1792.
(23) Lawrence, J. M.; Riseborough, P. S.; Parks, R. D. *Rep. Prog. Phys.* **1981**, *44*, 1–84.
(24) Mun, E. D.; Kwon, Y. S.; Jung, M. H. *Phys. Rev. B* **2003**, *67*, 033103.

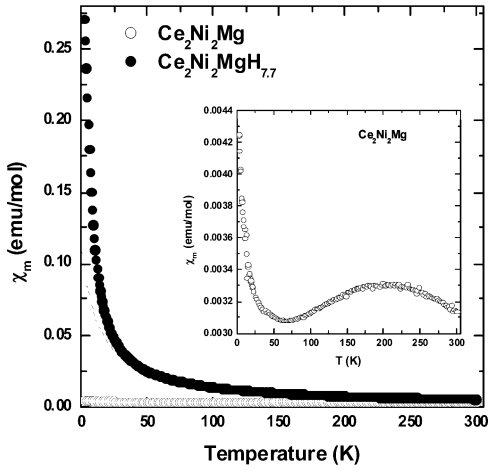


**Figure 5.** Temperature dependences of the magnetic susceptibility $\chi_m$ of $Ce_2Ni_2Mg$ and its hydride measured in an applied field of $H = 4$ T (the dashed line indicates the Curie−Weiss law (see text)). A zoom of $\chi_m = f(T)$ for $Ce_2Ni_2Mg$ is presented in the inset.

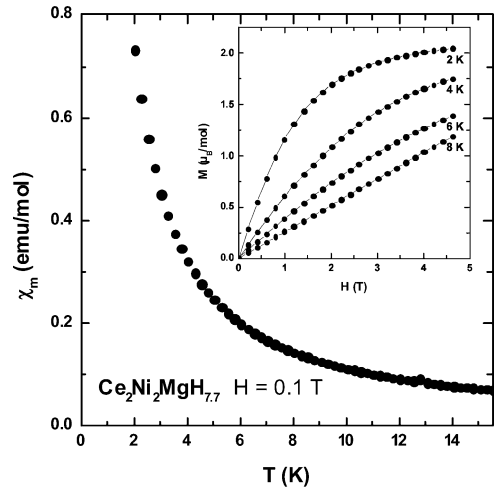


**Figure 6.** Temperature dependence ($T \leq 15.5$ K) of the magnetic susceptibility $\chi_m$ of $Ce_2Ni_2MgH_{7.7}$ measured with a field of 0.1 T. The inset presents the field dependence at low temperatures of the magnetization of the hydride.

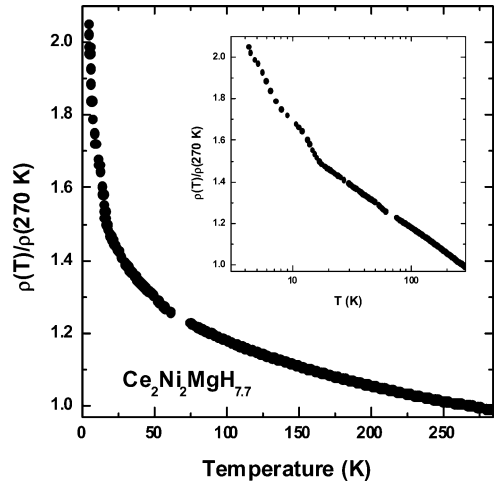


**Figure 7.** Temperature dependence of the reduced electrical resistivity of $Ce_2Ni_2MgH_{7.7}$. Inset: $\rho(T)/\rho(270\ K)$ as a function of log $T$.

susceptibility at $T = 0$ K, $n$ the proportion of stable $Ce^{3+}$ moments related to the trace of magnetic impurities, and $C = 0.807$ emu K/Ce-mol is the Curie constant for a free $Ce^{3+}$ ion. The best agreement between experimental and calculated $\chi_m$ values leads to $\chi_m(0) = 3.03 \times 10^{-3}$ emu/mol and $n = 5.65 \times 10^{-3}$ $Ce^{3+}$ ions/mol. Considering these values, the spin fluctuation temperature is determined as $T_{sf} = C/2\chi_m(0) = 133$ K resulting from the hybridization between 4f(Ce) and conduction electrons. This $T_{sf}$ temperature, smaller than that reported by Geibel et al.[15] ($T_{sf} \approx 250$ K), indicates that the coupling constant $J_{cf}$ is important in $Ce_2Ni_2Mg$.

On the contrary for the hydride $Ce_2Ni_2MgH_{7.7}$, above 50 K, the $\chi_m = f(T)$ curve follows a Curie−Weiss law with an effective magnetic moment $\mu_{eff} = 2.46$ $\mu_B$/Ce-mol and a paramagnetic Curie temperature $\theta_p = -14$ K. These values show (i) a trivalent state for Ce in this hydride, $\mu_{eff}$ is very close to that calculated for a free $Ce^{3+}$ ion (i.e., 2.54 $\mu_B$), and (ii) a weak influence of the Kondo effect since $\theta_p$ is small. This comparison suggests that the hydrogenation of $Ce_2Ni_2Mg$ leads to a valence transition of Ce from intermediate valence to $Ce^{3+}$ in the hydride.

No magnetic ordering can be clearly detected down to 1.8 K from the curve $\chi_m = f(T)$ giving the temperature dependence of the magnetic susceptibility measured at low field $H = 0.1$ T for the hydride $Ce_2Ni_2MgH_{7.7}$ (Figure 6). At low temperatures, the field dependence of the magnetization $M$ at 2 K (inset of Figure 6) exhibits a curvature toward the field axis, which could reveal the existence of some ferromagnetic correlations. At 2 K, no remanence is observed and the value of magnetization for $H = 4.6$ T is found to be approximately 1.02 $\mu_B$/Ce-mol. The curvature of the curves $M = f(H)$ decreases with increasing temperature and disappears above 8 K. This last behavior confirms the absence of any ferromagnetic nickel; this impurity was detected by magnetization measurements performed on the similar hydride $La_2Ni_2MgH_8$.[13]

The electrical resistivity of $Ce_2Ni_2MgH_{7.7}$ was measured on a bar compacted at room temperature, and, because of the presence of many porosities resulting from the preparation of the bar, absolute values of $\rho$(T) could not be determined accurately; for this reason, the reduced resistivity $\rho(T)/\rho(270\ K) = f(T)$ is reported here (Figure 7). However, to get a better understanding of the behavior of the hydride, we should make reference to similar measurements performed on the initial intermetallic $Ce_2Ni_2Mg$.[15] Its electrical resistivity decreases continuously from 300 down to 4.2 K but shows a pronounced curvature above 50 K. This last behavior, which deviates from that of a normal metal, is associated to the Kondo effect existing in the intermediate valence compounds.[25] On the contrary, the electrical resistivity of the hydride $Ce_2Ni_2MgH_{7.7}$ presents different characteristics; in the temperature range studied $\rho(T)$ increases with decreasing temperature. Above 15−20 K, the curve $\rho(T)/\rho(270\ K) = f(T)$ is characterized by incoherent Kondo scattering with a $\rho(T)/\rho(270\ K) = -A \log T$ ($A$ = constant) dependence (inset of Figure 7).[25] A sudden increase of $\rho(T)$ occurs below about 8−10 K. Similar behavior is observed for the ternary stannide CeNiSn which is considered a Kondo insulator

(25) Cornut, B.; Coqblin, B. *Phys. Rev. B* **1972**, *5*, 4541–4561.

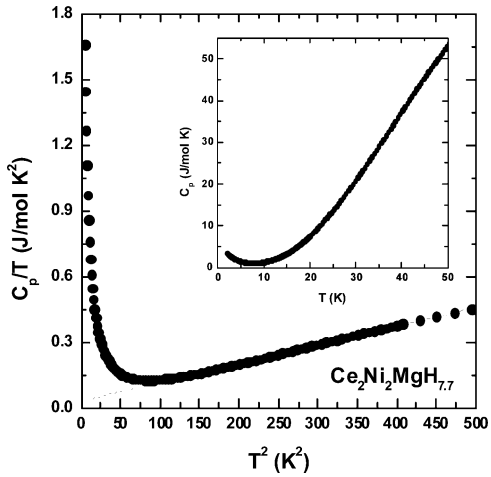


**Figure 8.** Specific heat $C_p$ divided by temperature $T$ versus $T^2$ for $Ce_2Ni_2MgH_{7.7}$ (the dotted line presents the fitting $C_p/T = \gamma + \beta T^2$ as indicated in the text). The curve $C_p = f(T)$ is plotted in the inset.

material.[6] The origin of this increase of $\rho(T)$ at low temperature may be explained since it appears also for the similar hydride based on lanthanum $La_2Ni_2MgH_8$.[13]

Finally, the hydride $Ce_2Ni_2MgH_{7.7}$ was investigated by specific heat measurements (Figure 8). No peak can be observed from the curve $C_p = f(T)$ (inset of Figure 8) in agreement with the absence of magnetic ordering down to 1.8 K as reported from the magnetization measurements. However, around 8−10 K, this curve exhibits an upturn attaining a value of 1.78 J/Ce-mol $K^2$ at 1.8 K suggesting that the hydride is a strongly correlated electron system at low temperature. This upturn is detected in the temperature range where the sudden increase of the electrical resistivity is evidenced and where the ferromagnetic correlations are detected by magnetization measurements. These behaviors suggest a modification of the interaction between the 4f(Ce) electrons and those of the conduction band near 8−10 K. At higher temperature between 10 and 22 K, a rather small electronic coefficient $\gamma$ can be obtained by fitting the data to the expression $C_p/T = \gamma + \beta T^2$ with $\gamma$ =15 mJ/Ce-mol $K^2$ and $\beta = 4.27\ 10^{-4}$ J/Ce-mol $K^4$ (Figure 8).

## Conclusion

The magnetization, electrical resistivity, and specific heat measurements presented here for $Ce_2Ni_2MgH_{7.7}$ indicate that this hydride does not show detectable long-range magnetic ordering down to 1.8 K. However, this study reveals at low temperatures some characteristic features of a non-magnetic strongly correlated electron system: the existence of ferromagnetic correlations and an important increase of its electrical resistivity and specific heat at low temperatures. These results confirm that the negative pressure produced by hydrogen insertion in intermetallics based on cerium is an interesting way to obtain new strongly correlated electron compounds.

**Acknowledgment.** This work was financially supported by the Deutsche Forschungsgemeinschaft. B.C., E.G., and R.P. are indebted to EGIDE and DAAD for research grants within the Procope programs (11457RD and D/0502176). Finally, B.C. thanks the European Science Foundation (ECOM-COST action P16) for financial support.

IC801076B